

# Proton transfer dynamics in the nonhomogeneous electric field of a protein

Ruth Yam,\* Esther Nachliel,\* Smadar Kiryati,\* Menachem Gutman,\* and Dan Huppert†

\*Laser Laboratory for Fast Reactions in Biology, Department of Biochemistry, Tel Aviv University, Tel Aviv; and †Beverly and Raymond Sackler Faculty of Exact Sciences, School of Chemistry, Tel Aviv University, Tel Aviv, Israel

**ABSTRACT** By adsorption of pyranine (8 hydroxypyrene 1, 3, 6 trisulfonate) to lysozyme we create on the positively charged protein a fluorophoric site with a total charge of  $-3$ . Photo dissociation of the dye's hydroxyl proton changes its absorption and fluorescence spectrum, permitting a continuous monitoring of the reprotonation dynamics. Absorbance measurements in the microsecond time scale monitor how the bulk protons penetrate the Coulomb cage of the bound dye. Time-resolved fluorescence monitors how the proton is escaping out of the Coulomb cage of the bound dye.

These probe reactions were studied with a series of dye-enzyme complexes where the number of free carboxylate was reduced by amidation, increasing the total charge of the complex from  $+5$  to  $+12.6$ .

The time-resolved measurements demonstrate the complexity of the electric field in the immediate vicinity of the dye. It is consistent with a negative potential wall (of the anion) surrounded by a positive potential wall of proteinaceous moieties.

## INTRODUCTION

The electric field surrounding a protein affects its equilibrium and dynamic properties. The interaction energy with any ion in solution is affected by the sum of forces applied, at the ion coordinates, by all charges and permanent dipole of the protein. Consequently, the probability of an ion to approach a given site on the protein is a function of the potential field in the solvent (Getzoff et al., 1983). The paramount importance of this concept is illustrated by the number of reviews published in a single review journal in the past 5 y (Matthew, 1985; Honig et al., 1986; McLaughlin, 1989).

The effect of the total electric charge on the ionization potential of proteins is calculated by the Tanford Kirkwood equation (1957) which is solved simultaneously for all charges and permanent dipoles. This procedure necessitates an accurate three-dimensional positioning of all charged moieties and quantitation of the solvent accessibility of each site. With this data at hand the interaction potential of every site with a charged ion can be calculated. The analysis, in most cases, is aimed at reconstructing the total charge ( $Z_{tot}$ ) vs. pH curve, and its dependence on the ionic strength. The validity of the analysis is confirmed by comparison of the measured pK (or  $pK_{1/2}$ ) values with those predicted by the theoretical calculations, as exemplified by Matthew et al. (1979) or Spassov et al. (1989). Naturally, the Kirkwood Tanford analysis necessitates the detailed information derived from crystal x-ray analysis of a protein. It cannot be operated in the reverse direction, to guess from the pK

measurement in which environment the observed group is.

This shortcoming can be circumvented by monitoring the dynamics of proton interaction with the site. The rate of proton binding is affected by electrostatic attraction-repulsion forces, which can direct the motion of the proton into energetic preferential trajectory: for example, the electrosteering of the superoxide anion to the active site of the superoxide dismutase (Honig et al. 1986).

At a long distance from the protein (due to protein rotation and damping of the electric force by the dielectric screening of water) an ion will respond to the protein charge as if it is a point charge. At close distance the electric field around the enzyme lobes forms a funnel leading the substrate to the active site (Getzoff et al., 1983; Klapper et al., 1986; Head-Gordon and Brooks, 1987).

The kinetic effect of an inhomogeneous electric field is characterized by two features: (a) The rate constant of the ligand interaction with the site will deviate from the rate predicted for a diffusion-controlled reaction (calculated for uncharged reactants) while the activation energy is typical for diffusion controlled reactions.

(b) The screening effect of a salt will contradict that expected according to the charge product ( $z_1 z_2$ ) of the reactants. Cudd and Fridowich (1982) noted that the rate of catalysis of superoxide dismutase is decelerated upon increasing the ionic strength of the solution. This observation contradicts the repulsive force between the net charge of the enzyme ( $z_1 = -4$ ) and the substrate

Address correspondence to Dr. Gutman.

( $z_2 = -1$ ). Consequently, it was proposed that a positive charge near the active site caused a local attractive force between the site and substrate.

The theoretical calculations of Honig and co-workers (Klapper et al., 1986) (based on precise assignment of charges on the protein surface) and those of Head-Gordon and Brooks (1987) (based on monopole and quadrupole truncation of the 76 charges dispersed on the protein's surface) led to similar conclusions. The electric field around the superoxide dismutase has two (negative) repulsive lobes which repel the ligand and two (positive) attractive channels through which the anion is attracted to the active site. When the ionic screening is increased, it blocks the attractive channels, as is common for all anion-cation interaction.

The dynamic studies described above were based on simulated Brownian trajectories (see Head-Gordon and Brooks, 1987, and references therein). Imaginary "particles" are formed in a computation space at a given distance from a fixed charged "body" of a known electric field and their "diffusion trajectory" is monitored. The process is quantified by the fraction of trajectories which ended at the "active region" of the target. The present publication describes time-resolved experimental measurements of proton kinetics with a protein bound chromophore.

The experimental system consists of an excited-state proton emitter, pyranine (8 hydroxy pyrene 1, 3, 6 trisulfonate) adsorbed to the positively charged protein lysozyme. When the dye is photoexcited to the first excited electronic singlet state it shifts its  $pK$ , becoming a very strong acid and the hydroxy proton dissociates with a time constant of  $\approx 100$  ps (Gutman, 1986). In that system a short laser pulse synchronizes a massive proton dissociation and detectable populations of anions are formed. In our experiments we monitor the recombination of the protons with the parent anions using either time-resolved fluorometry (monitoring the dynamics within the first 2 ns after excitation) or transient absorption spectroscopy for following the events until the final relaxation of the perturbation.

The dynamic measurements were carried out using either a native protein dye complex or complexes with modified enzyme (where the carboxylates groups were amidated), thus increasing the total positive charge of the complex (Carraway and Koshland, 1972).

Our measurements demonstrate that the length of the time window affects the apparent nature of the observations. Measurements in the microsecond scale monitor the recapture of a bulk proton by the protein-bound dye. When the positive charge of the protein was increased by amidation, the local electrical field repulsed the proton leading to a slower reaction. The subnanosecond dynamics monitor the attempt of the proton to escape

from the Coulomb cage of the excited anion (Pines et al., 1988). In this case the incremental positive charge of the protein hinders the escape of the proton, indicating an effective positive potential wall surrounding the (negative) potential well of the excited anion.

## MATERIALS AND METHODS

Pyranine (8 hydroxy pyrene 1, 3, 6 trisulfonate), laser grade, was supplied by Kodak. Lysozyme (chicken egg white, grade I) was purchased from Sigma. Glycine amide (HCl) and EDC (EDC, (1-ethyl-3-(3-dimethylaminopropyl)carbodiimide)) used for amidation were by Aldrich and Sigma, respectively.

Steady state fluorescence measurements were carried out using Shimadzu RF 540 spectrofluorimeter with background correction. Time-resolved fluorescence measurements were carried out in the system described by Pines et al. (1988). Transient absorbance kinetics and their analysis were carried out as described by Gutman (1986) and Yam et al. (1988).

Amidation of carboxylate moieties of lysozyme was executed as described by Carraway and Koshland (1972). The enzyme (8 mg/ml) was dissolved in 1 M glycine amide hydrochloride at  $pH = 4.75$ . The carbodiimide derivative EDC was added as solid to a final concentration of 0.1 M while maintaining a constant pH by manual addition of 1 M HCl. The reaction was terminated at the desired time by addition of acetate buffer ( $pH = 4.75$ ) to a final concentration of 1.6 M. The protein was dialyzed ( $4^\circ C$ ) against water before use.

## RESULTS

### Binding of pyranine to lysozyme

Adsorption of pyranine to lysozyme is associated with intensified steady state emission of the undissociated dye ( $\Phi OH^*$ ). This is seen as the enhanced band at 440 nm shown in the insert to Fig. 1 (*curve A vs. B*). Similar enhancement of  $\Phi OH^*$  emission was recorded in other systems of adsorbed dye, like bovine serum albumin (Gutman et al., 1982a), Apomyoglobin (Gutman et al., 1982b) or when adsorbed to phosphatidylcholine membranes (Nachliel, unpublished results).

The binding of pyranine to the lysozyme, as revealed by the fluorescence emission, is pH sensitive. A group with  $pK = 6.3 \pm 0.1$  must be protonated to bind the dye. As this moiety is more acidic than the bound dye ( $pK = 7.45 \pm 0.05$ ), the pH dependence of binding is attributed to protonation of a proteinaceous group. The amidation of the solvent accessible carboxylates of lysozyme better resolves the role of this moiety in binding and a  $pK = 6.3 \pm 0.1$  is measured. On this basis we conclude that the bound dye is in its  $\Phi OH$  form and one of the anchoring groups has a  $pK = 6.3 \pm 0.1$ .

The binding of pyranine to lysozyme follows a saturation curve, corresponding with a 1:1 complex with an association constant of  $15.7 \cdot 10^6 M^{-1}$  (see Fig. 1).

The protein dye complex is mostly electrostatic. Addi-

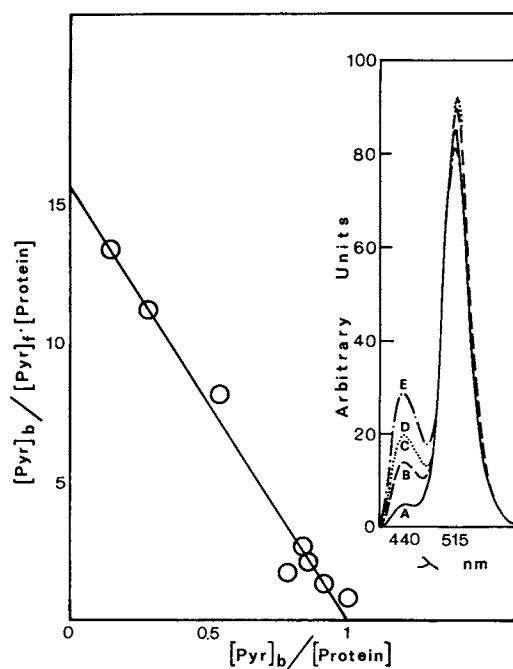


FIGURE 1 Scatchard plot for the binding of pyranine to lysozyme. The binding was monitored fluorometrically from the emission spectra of pyranine in presence of lysozymes and quantitated by the ratio of the shortwave length emission ( $\lambda = 440$  nm) of  $\Phi\text{OH}^*$  to the long wavelength emission ( $\lambda = 515$  nm) of  $\Phi\text{O}^{*-}$  (insert). The analysis was carried out as detailed by Gutman et al. (1982b). The reaction was at pH = 5.5 with  $0.5 \mu\text{M}$  lysozyme and varying concentration  $0.05$ – $5 \mu\text{M}$  of the ligand. The curves in the insert are the emission spectra of pyranine in water (A) and lysozyme-pyranine complexes with (B) native enzyme and enzymes subjected to amidation of carboxylate for 15 min (C), 40 min (D) and 180 (E). Excitation wavelength at 400 nm.

tion of low concentration of electrolyte weakens the binding, as shown in Fig. 2 and in Table 1.

### The effect of carboxylate amidation on the lysozyme pyranine complex

Blocking the carboxylates of lysozyme does not prevent the binding of the dye. On the contrary, the complex is more stable. The concentration of salt needed to reduce the enhanced emission of  $\Phi\text{OH}^*$  by 50% increases with the extent of carboxylate neutralization. Protein subjected to exhaustive treatment binds the dye so avidly that 120 mM NaCl are needed to lower the incremental emission to half. In comparison only 5 mM NaCl are required to have a similar effect on native enzyme-dye complex (see Table 1).

As binding of dye still requires the protonation of the  $\text{pK} = 6.3$  moiety, we conclude that native and modified protein bind the dye at the same site.

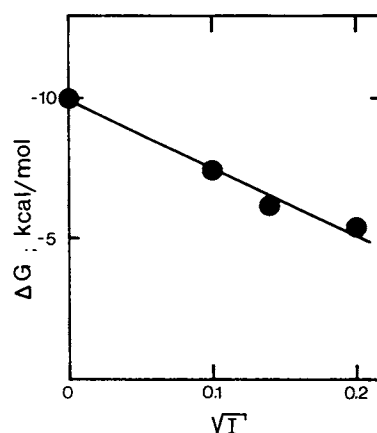


FIGURE 2 The effect of ionic strength on the association energy of the lysozyme (native) pyranine complex. The titrations were measured as in Fig. 1, in the presence of varying concentrations of NaCl.

Amidation of the solvent accessible carboxylates increases the net positive charge of the protein with subsequent shift of the  $\text{pK}$  of the adsorbed dye (see Table 1, column 1). The  $\text{pK}$  shift of the adsorbed dye was attributed to the total charge increment of the protein as given by the equation

$$\Delta\text{pK}_{\text{int}} = 0.868 \cdot W \cdot \Delta Z, \quad (1)$$

where  $W$  is the electrostatic work associated with charging a body, of radius  $Rm$ , dissolved in water ( $\epsilon = 78.3$ ) (Tanford, 1955).

$$W = \frac{e_0^2}{2\epsilon RmkT} \cdot \frac{1}{1 + Rmk} \quad (2)$$

( $e_0$  is the electron charge and  $\kappa$  is the Debye length). For lysozyme at diminishing small ionic strength  $W = 0.205$ .

Using this value we calculated the incremental charge of the protein gained by amidation (see Table 1).

TABLE 1 The effect of carboxylates neutralization on the lysozyme-pyranine complex

Modification time	$\text{pK}$	$\Delta\text{pK}$	$\Delta Z^*$	$Z^\dagger$	NaCl <sup>‡</sup>	$\frac{I(\Phi\text{OH})^*}{I(\Phi\text{O})^{*-}} \%$
<i>min</i>					<i>mM</i>	
0	$7.45 \pm 0.05$	—	—	9.0	5	14
15	$6.5 \pm 0.05$	0.95	5.3	14.3	15	22.2
45	$6.3 \pm 0.15$	1.15	6.5	15.5	80	21
180	$6.1 \pm 0.05$	1.35	7.6	16.6	120	24

\*The charge increment was calculated according to Tanford (1957).

†Total charge was taken as that of neutral protein at pH = 5.5 plus the charge increment,  $\Delta Z$ , calculated in column 4.

‡The concentration of salt needed to reduce the incremental emission to half.

Protein sample subjected to 3 h amidation shifted the  $pK_{\text{int}}$  of the dye by 1.35 pK units, which correspond with incremental charge of  $\Delta Z = +7.6$ . This value is in good agreement with the yield of amidation done under the same conditions (Carraway and Koshland, 1972). Equilibrium parameters correspond with a long (or infinite) observation time, thus protons far from the dye can interact with it. In this regime we find that a centrosymmetric presentation of the charge corresponds well with the measured properties of the protein.

### Gauging the outer perimeter of the Coulomb cage of the bound dye

In a diffusion controlled reaction, the rate-limiting step in product formation is the approach of the two reactants to a contact radius ( $r_o$ ).

If the reactants are interacting electrostatically a new term is introduced: the Debye radius. It is the distance where the electric potential energy equals the thermal energy.

$$R_D = |Z_1 \cdot Z_2| \frac{e_o^2}{\epsilon kT} \quad (3)$$

for aqueous solution  $R_D = 7 \cdot |Z_1 Z_2|$  (given in ångströms  $\delta$ ).

To avoid ambiguities emerging from negative values due to  $Z_1 Z_2 < 0$  it is more convenient to use the expression  $\delta = R_D / r_o$ , which is the ratio between the Debye radius and the radius of contact has the proper sign of the charge product and can be either positive or negative.

The contribution of the electrostatic force to the rate constant of the reaction is expressed by the Debye Smoluchowski equation which at diminishing ionic strength is given below.

$$k_{DC} = k_{en} \delta / [\exp(\delta) - 1], \quad (4)$$

where  $k_{en}$  is the rate of encounter between uncharged reactants. This rate of encounter, between a ligand and a reactive patch on a rotating protein, was calculated according to Shoup et al. (1981). Consequently, if  $k_{DC}$  is measurable,  $k_{en}$  is calculable, and  $r_o$  is known, one can determine by Eqs. 3 and 4 what is the effective charge product for binding a proton coming from the bulk.

To measure the effective charge controlling the reaction between the bound anion and a free proton, we employed a short laser pulse to drive the proton from the bound dye (Gutman, 1986) and subsequently measured the rate of reprotonation of the adsorbed anionic dye  $\Phi O^-$  (see Fig. 3).

The excitation was by a 10-ns laser pulse and the

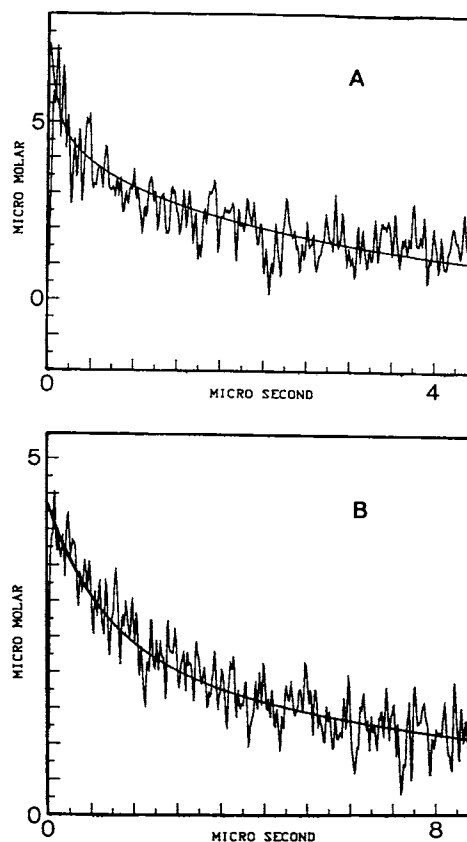


FIGURE 3 Time-resolved measurement of the pyranine anion reprotonation in the dye lysozyme complex. The complex (20  $\mu\text{M}$  dye in 100  $\mu\text{M}$  lysozyme) was excited by a short laser pulse ( $\lambda = 337$  nm, 10 ns full width at half maximum) which photodissociated the proton leaving the anion ( $\Phi O^-$ ) bound to the protein. The reprotonation was monitored at  $\lambda = 457$  nm ( $\epsilon = 24,000 \text{ M}^{-1} \text{ cm}^{-1}$ ). The experimental signal is a time-resolved average of 512 successive excitation pulses delivered at a rate of 10 pps. The continuous curve is a simulated dynamic using the differential rate equation given in Yam et al. (1988). (A) Dynamics of reprotonation of pyranine native-lysozyme complex. (B) Dynamics of reprotonation of dye adsorbed on enzyme subjected to amidation for 180 min. Note changes in ordinate and abscissa scales.

reaction was followed at a wavelength where the ground state anion ( $\Phi O^-$ ) has a strong absorbance ( $\epsilon_{457} = 24,000 \text{ M}^{-1} \text{ cm}^{-1}$ ).

The discharged protons interact with two classes of protein. To the first class we assign the pyranine-free protein and those pyranine-enzyme complexes where the dye has not ejected its hydroxyl proton. With respect to our monitoring system this class is "transparent". We cannot detect its protonation directly, only to deduce its dynamics by the global analysis.

The second class contains the dye-protein complexes which lost their proton by the photochemical reaction. The reprotonation of these dye molecules is the experi-

mentally measured parameter. The analysis of the dynamics includes the two classes of the protein, and dissects the process into many discrete chemical reactions as described by Yam et al. (1988). A set of nonlinear coupled differential equations are written, representing all the reactions taking place, with their appropriate equilibrium and rate constants. A single set of constants is looked for, which reproduces the observed dynamics, as measured with native and modified protein complexes.

Fig. 3, *A* and *B* depicts the measured dynamics (for native and exhaustively modified protein) and the simulated dynamics.

Amidation of the protein increased the charge of the complex from +5 up to +12.6, yet the effect on the rate constant of the proton-dye reaction is much milder. The ratio between the measured rate constant and the rate of encounter, calculated according to Shoup et al. (1981) (see Table 2, 4th column) decreases from 1.6 to 0.48. The value of  $\delta$  (see Eq. 4) and the corresponding effective charge (through Eq. 3) ( $Z_{\text{eff}}$ ) are calculated and given in the table.

The unmodified protein complex with pyranine has a total charge of +5. With respect to the proton binding dynamic, there is an effective charge of  $-1$  steering the proton to  $\Phi\text{O}^-$ . Neutralization of the carboxylates increases the net charge of the complex to +12.6. Yet with respect to the dynamics, the charge affecting the rate constant is only +1.2.

Thus we conclude that the rate constant of the reaction is determined not by the total charge of the protein but by the effective potential operating near the observed site.

TABLE 2 Rate constants of protonation of pyranine anion on native and modified lysozyme

Modification time	$k_{\text{DC}}^*$	$Z^{\dagger}$	$\frac{k_{\text{DC}}^{\ddagger}}{k_{\text{en}}}$	$\delta^{\S}$	$Z_{\text{eff}}^{\P}$
<i>min</i>	$10^{10} \text{ M}^{-1} \text{ s}^{-1}$				
0	$10.0 \pm 0.3$	+5	1.6	-1.05	-1
15	$6.25 \pm 0.25$	+10.3	1.01	0	0
40	$4.25 \pm 0.25$	+11.5	0.68	0.68	+0.65
180	$3.0 \pm 0.2$	+12.6	0.48	1.3	+1.23

\*As obtained from simulated dynamics exemplified in Fig. 3. The rates were measured at low ionic strength  $I < 10^{-3}$ .

$^{\dagger}$ The charge of protein-pyranine anion. Taken as that calculated according to Tanford and tabulated in Table 1 adjusted by the  $-4$  charge of the dye.

$^{\ddagger}$  $k_{\text{en}}$  encounter was calculated according to Shoup (1981), correcting for the rotational diffusion of the protein.

$^{\S}$ Calculated as explained in the text.

$^{\P}$ The effective charge corresponding with the measured dimension of the Coulomb cage  $Z = \delta \cdot R_0 \epsilon kT/e_0^2$  assuming  $\epsilon = 78$ .

## Gauging the electrostatic cage of adsorbed pyranine by an inside proton

A positively charged Coulomb cage evicts a proton very rapidly, driving it out both by diffusion and by electrostatic repulsion. Accordingly, we expect that increasing the effective charge of the site will accelerate the escape of proton to the bulk. This is contrary to the observation (Fig. 1, curves *B–D* in insert and Table 1, last column). The more positive complex exhibits the strongest emission of the undissociated pyranine ( $\Phi\text{OH}^*$ ). This is indicative of a case where the probability of proton to escape from the Coulomb cage of the bound dye  $\Phi\text{O}^{*-}$  is lower than from a dye in bulk water.

A time-resolved fluorescence curve of  $\Phi\text{OH}^*$  emission is shown in Fig. 4. Curve *A* was measured with free pyranine in water. It is characterized by two features: a fast initial decay ( $\tau \approx 100$  ps) followed by a long shallow tail. This tail, formed by geminate recombination taking place in the Coulomb cage, represents that fraction of the proton population which fails to diffuse out of the cage (Pines et al., 1988). As seen in curve *B* (Fig. 4), the binding of the dye to lysozyme enhances the magnitude of the tail. Curve *C*, measured with dye-modified protein complex, features an even slower fluorescence decay.

The inflated tail structure seen in curves *B* and *C* is

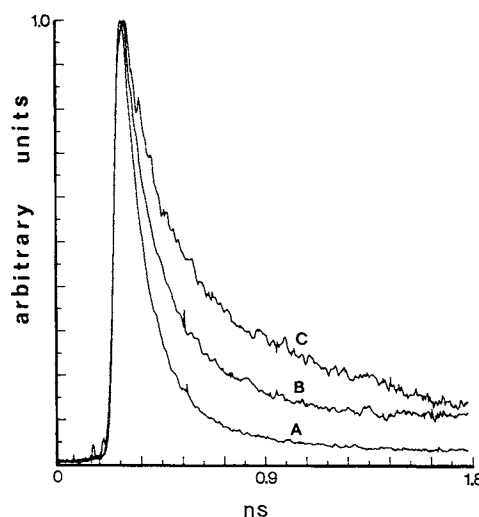


FIGURE 4 Time-resolved fluorescence emission of  $\Phi\text{OH}^*$  adsorbed on lysozyme. The dye was excited by the third harmonics of a Yag laser ( $\lambda = 355$  nm, 25 ps full width at half maximum) and the emission of  $\Phi\text{OH}^*$  was monitored by a streak camera and multichannel analyzer as described by Pines et al. (1988). Curve *A* was measured with 45  $\mu\text{M}$  of dye, dissolved in water (pH = 5.4). Curve *B* was measured with 45  $\mu\text{M}$  of dye in the presence of 270  $\mu\text{M}$  of native enzyme. Curve *C* was measured with 45  $\mu\text{M}$  of dye and 140  $\mu\text{M}$  of enzyme subjected to amidation conditions for 180 min.

due to a combination of two mechanisms, enhanced recombination, and a slower dissociation of the proton after each recombination event.

To differentiate between the two factors, we used the expression of Pines and Huppert (1989) which relates the steady state fluorescence emission ratio ( $I_{440}/I_{515}$ ), the time constant of initial dissociation ( $\tau_d$ , measured from the initial part of the fluorescence decay) and the fluorescence lifetime of  $\Phi\text{OH}^*$  ( $\tau_{\Phi\text{OH}} = 5.5$  ns).

$$NR = [\tau_{\Phi\text{OH}}(I_{440}/I_{515})]/\tau_d^{-1} \quad (5)$$

This expression provides the average number ( $NR$ ) of recombinations of a proton with its parent excited anion before it decays to the ground state.

Table 3 summarizes the result of these calculations. The initial dissociation time of a proton from free pyranine is  $120 \pm 10$  ps (Pines and Huppert, 1989). This time constant is stretched to a  $\approx 170$  ps when the dye is bound to a protein and to  $\approx 230$  ps if the carboxylates are amidated. The slower rate of deprotonation is attributed to unavailability of water molecules needed to stabilize the proton by hydration (Huppert et al., 1982). The slower rates of the initial fluorescence decay, as observed in curves *B* and *C*, imply that the water in the hydration layer of the protein has a lower activity than the bulk water. The activity of water in the immediate vicinity of the pyranine binding site on lysozyme is listed in Table 3. The charged protein interacts with the hydration layer making the water molecules less available for hydrating the proton. The highly charged protein (+12.6) affects the water more than the native one.

In conjunction with the decrease of the dissociation rate, we observe an increase in the number of recombinations. While in bulk water an average  $\Phi\text{O}^*$  proton pair experiences 1.5 recombinations, the protein adsorbed dye undergoes 2.7 recombinations. On the extracharged protein it is almost 4. Thus, contrary to our expectations, the escape from the Coulomb cage of the anion, ad-

sorbed to a positively charged protein, is more difficult than from the cage of a free anion. This can be explained by the immediate presence of positive charges surrounding the anion, forming a high (repulsive) potential wall which prevents the proton escape from its negative (attractive) potential well.

## DISCUSSION

In this study we established an experimental model system suitable for evaluating the electric field at a defined site on a protein in solution.

The method is based on dynamic measurement of a well-understood reaction: the diffusion-controlled reaction of a proton with an anion in dilute aqueous solution. These measurements were carried out in two kinetic regimes: the first one is the homogeneous reaction of a proton with a dye. In this case the proton concentration is constant in the total volume and "consumed" upon entering the Coulomb cage around the dye. The second regime is geminate recombination. In this case the probability of finding a free proton within the Coulomb cage is higher than in an equal volume in the bulk. The relaxation of this transient state is by proton escape to the bulk. Through this mechanism the geminate recombination system evolves with time to the homogeneous reaction. Both geminate and homogeneous reactions are suitable for a quantitative analysis of the experimental results.

The electric charge of the protein was increased by amidation of the free carboxylates of the protein. These groups are not directly involved in the binding of the dye.

Equilibrium measurement revealed a good agreement between the incremental charge ( $\Delta Z = +7.6$ ) and the number of carboxylates susceptible to the amidation, 7-8, (Carraway and Koshland, 1972) (see Table 1). This agreement is not apparent in dynamic measurements, as if the calculated charge varies with the observation time. This apparently unacceptable conclusion is self-explanatory if we consider the nature of the measurement event. In one case (Table 2) we monitor the encounter of a proton homogeneously distributed in bulk water, with the outer surface of the Coulomb cage. In the second system (Table 3) we observe the reverse reaction, the escape of the proton from the electrostatic cage, diffusing against the electrostatic force.

## Dynamics of the homogeneous reaction

The rate-limiting step of diffusion-controlled protonation is the encounter of the proton with the outer

TABLE 3 Kinetic parameters of proton dissociation, recombination within the Coulomb cage of excited pyranine bound to lysozyme

<i>Z</i> (total)	$k_{\text{diss}}^*$	$a_{\text{H}_2\text{O}}^\dagger$	$NR^\ddagger$
	ps		
free	$120 \pm 10$	1.0	1.5
+5	$167 \pm 10$	0.94	2.73
+12.6	$227 \pm 15$	0.915	3.9

\*Measured by convolution procedure.

†Calculated according to Gutman et al. (1982a, b).

‡Calculated according to Pines and Huppert (1989).

perimeter of the Coulomb cage. Once the proton is within this space the covalent bond will be formed within a nanosecond or less. This fact makes it possible to gauge the size of the electrostatic cage by analyzing the rate constant of the reaction according to Debye Smoluchowski equation. In the same way it can be used for calculating the effective charge of the cage. The charge affecting the rate of proton binding to the adsorbed pyranine is  $-1$  (see Table 2). This charge is less than the  $-4$  of the free anion. Most of it is neutralized or screened by the positive charges anchoring the anion. We can assume that the dye is bound by salt bridges between its three sulfonate groups with three positive charges (His  $-15$  may be one of them). In this state the dye region is unchanged while a net  $-1$  charge appears after the photodissociation of the hydroxyl's proton.

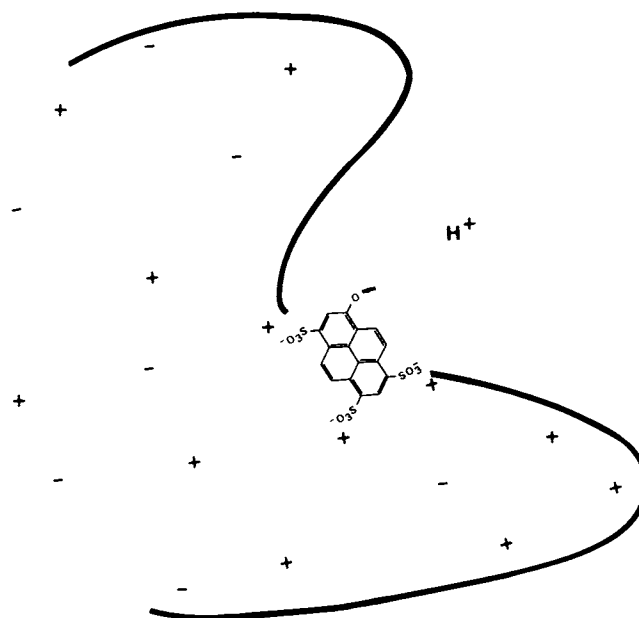
Neutralization of the protein's carboxylates increases its total charge, yet the effective field controlling the rate of the reaction varies from  $-1$  to  $+1.2$ , much less than the total increment of the protein-dye complex (from  $+5$  to  $+12.6$ ). This is an indication that the electric field around the protein, at a distance comparable with the Debye length (where the electric potential equals the thermal energy) deviates strongly from the centrosymmetric pattern. In the present case the neutralization of the negative carboxylates allows a better expression of the positive charges, leading to an effective repulsive force between the proton and the immediate surrounding of the oxy anion of the dissociated dye.

## Geminate recombination

Geminate recombination is measured under conditions where the probability of finding a proton at the immediate vicinity of the dye is higher than in the bulk. It is a precarious situation which vanishes rapidly as the proton diffuses to the bulk within a few nanoseconds or less.

The dynamics of geminate recombination in a spheric symmetric space, such as pyranine in bulk water (corresponding with curve *A*, Fig. 1) has been solved by Pines et al. (1988). This solution employs a numerical solution of the Debye Smoluchowski equations. The entire solution necessitates definition of microscopic molecular parameters such as rate constant of proton transfer from the dye to the water and the proton recombination rate on a reaction sphere radius. In our present case this analysis is not applicable as the boundary conditions and the potential field strength deviate from a spheric symmetric environment. On the other hand the average number of recombinations (NR) (Pines et al., 1988; Pines and Huppert, 1989) is a more lenient term and can be applied in our study.

The dissociation of proton from the bound pyranine is characterized by many recombination events, much



SCHEME 1

more than in bulk water (Table 3). Thus, we must account why the escape of a proton from apparently positive charged cage (lower row in Tables 1 and 2) is more difficult than from the electrostatic potential well made by  $-4$  charges as in the free dye (upper row in Table 3).

The enhanced recombination we noted in the present study reflects the distribution of charges within the Coulomb cage, the space operatively defined by the measurements carried out with "outside" proton (Table 2). Inside this space we find both the negative charges of the pyranine molecule and the anchoring positive charges of the protein. Thus the electric force operating on the dissociating proton is not only the attraction by the anion but also the repulsion by the surrounding positive charges. As the negative charges of the protein are neutralized by amidation, the effective local positive field around the pyranine is more intensive, redirecting the proton toward the anion; see scheme 1.

At a molecular level the electrostatic interactions are effective whatever the observation techniques are. It is the macroscopic reflection of these forces which appear to vary. In this study we demonstrated how by varying the observation period we can zoom in on the fine details of the nonrandom architecture of electric charges of a protein molecule in solution.

This research was supported by the United States-Israel Binational Science Foundation (87-0035) and the US Navy, Office of Naval Research (N00014-89-J-1622).

---

Received for publication 12 March 1990 and in final form 23 July 1990.

---

## REFERENCES

- Carraway, K. L., and D. E. Koshland Jr. 1972. Carbodiimide modification of proteins. *Methods Enzymol.* 25:616–623.
- Cudd, A., and I. Fridovich. 1982. Electrostatic interaction in the reaction mechanism of bovine erythrocyte superoxide dismutase. *J. Biol. Chem.* 257:11443–11447.
- Getzoff, E. D., J. A. Tainer, P. K. Weiner, P. A. Kollman, J. A. Richardson, and D. C. Richardson. 1983. Electrostatic recognition between superoxide and copper, zinc superoxide dismutases. *Nature (Lond.)* 306:287–290.
- Gutman, M. 1986. Application of the laser induced proton pulse for measuring the protonation rate constants of specific sites on protein and membranes. *Methods Enzymol.* 127:522–538.
- Gutman, M., D. Huppert, and E. Nachliel. 1982a. Kinetic studies of proton transfer in the microenvironment of a binding site. *Eur. J. Biochem.* 121:637–642.
- Gutman, M., E. Nachliel, and D. Huppert. 1982b. Direct measurements of proton transfer as a probing reaction for the microenvironment of the apomyoglobin heme binding site. *Eur. J. Biochem.* 125:175–181.
- Head-Gordon, T., and C. L. Brooks. 1987. The role of electrostatics in binding of small ligands to enzymes. *J. Phys. Chem.* 91:3342–3349.
- Honig, B., W. L. Hubbell, and R. F. Flewelling. 1986. Electrostatic interaction in membrane and protein. *Annu. Rev. Biophys. Biophys. Chem.* 15:163–193.
- Huppert, D., E. Kolodney, M. Gutman, and E. Nachliel. 1982. Effect of water activity on the rate of proton dissociation. *J. Am. Chem. Soc.* 104:6949–6953.
- Klapper, I., R. Hagstrom, R. Fine, K. Sharp, and B. Honig. 1986. Focusing of electric fields in the active site of Cu-Zn Superoxide Dismutase:  $\epsilon$  effects of ionic strength and amino acid modification. *Proteins Struct. Funct. Genet.* 1:47–49.
- Matthew, J. B. 1985. Electrostatic effects in proteins. *Annu. Rev. Biophys. Biophys. Chem.* 14:387–417.
- Matthew, J. B., G. I. H. Hannania, and F. R. N. Gurd. 1979. Electrostatic effects in hemoglobin hydrogen ion equilibria in human deoxy and oxyhemoglobin A. *Biochemistry* 18:1919–1928.
- McLaughlin, S. 1989. The electrostatic properties of membranes. *Annu. Rev. Biophys. Biophys. Chem.* 18:113–136.
- Pines, E., and D. Huppert. 1989. Salt effect in photoacids quantum yield measurements: a demonstration of the role of geminate recombination in deprotonation reactions. *J. Am. Chem. Soc.* 111:4096–4097.
- Pines, E., D. Huppert, and N. Agmon. 1988. Geminate recombination in the excited state proton transfer reactions: numerical solution of the Debye Smoluchowski equation with back reaction and comparison with experimental results. *J. Chem. Phys.* 88:5620–5630.
- Shoup, D., G. Lipari, and A. Szabo. 1981. Diffusion controlled bimolecular reaction rates. The effect of rotational diffusion and orientation constraints. *Biophys. J.* 36:697–714.
- Spassov, V. Z., A. D. Karshikow, and B. P. Atanasov. 1989. Electrostatic interactions in proteins: a theoretical analysis of lysozyme ionization. *Biochim. Biophys. Acta.* 999:1–6.
- Tanford, C. 1955. The electrostatic free energy of globular proteins in aqueous salt solution. *J. Phys. Chem.* 59:788–793.
- Tanford, C., and J. G. Kirkwood. 1957. The theory of protein titration curves. I. General equations for impenetrable sphere. *J. Am. Chem. Soc.* 79:5333–5339.
- Yam, R., E. Nachliel, and M. Gutman. 1988. Proton-protein interaction. *J. Am. Chem. Soc.* 110:2636–2640.